Molecular BioSystems

PAPER

View Article Online
View Journal | View Issue

Cite this: *Mol. BioSyst.*, 2014, **10**, 1940

Quantitative proteomic analysis reveals mitochondrial protein changes in MPP$^+$-induced neuronal cells†

Jee Won Choi,[a] Min-Young Song[a] and Kang-Sik Park*[ab]

Received 15th January 2014,
Accepted 18th April 2014

DOI: 10.1039/c4mb00026a

www.rsc.org/molecularbiosystems

Parkinson's disease (PD) is a common neurodegenerative disorder pathologically characterized by the loss of dopaminergic neurons in the substantia nigra pars compacta. To further explore potential functional mechanisms of PD, we performed a comparative proteomic analysis using stable isotope labeling with amino acids in cell culture (SILAC) combined with nano-LC tandem mass spectrometry (nano-LC MS). In total, 1740 proteins were identified in MPP$^+$-treated SH-SY5Y cells. Our comparative proteomic analysis indicated that a total of 39 proteins were differentially expressed in SH-SY5Y cells responding to MPP$^+$ treatment. Of these, 14 altered proteins were clustered in the mitochondria, 5 proteins were already reported as related to PD, and the remaining proteins were newly identified in this study. Together, our data further define that the mitochondria play an important role in regulating PD through multiple and complex mechanisms and provide new insights into the functional contribution of mitochondrial proteins in PD.

Introduction

Parkinson's disease (PD) is the second most common neurodegenerative disorder and is pathologically characterized by the loss of dopaminergic neurons in the midbrain substantia nigra pars compacta and by the accumulation of Lewy bodies containing α-synuclein.[1] This dopamine loss causes prominent clinical motor symptoms, such as bradykinesia, resting tremor, rigidity and postural instability.[2] Research over the past few decades has been focused on identifying genetic mutations that are associated with familial PD, including α-synuclein, Parkin, PINK1, LRRK2, and DJ-1, *etc.*[3,4] On the other hand, a majority of the disease cases (90%) are sporadic PD, which seems to arise from complex interactions between environmental exposure and genetic susceptibility.[5]

A number of studies have reported that mitochondrial dysfunction and oxidative stress are linked to PD.[2,5,6] Mitochondrial dysfunction with complex I deficiency and inhibition of the electron transfer chain system are involved in PD.[1,7] Moreover, reactive oxygen species (ROS) activity has been suggested as one of the mechanisms for the death of dopaminergic neurons in PD, and mitochondrial complex I is considered to be one of the main sources of ROS.[5,6] Mutations in mitochondrial proteins have been associated with familial PD.[8] Environmental toxins, such as 1-methyl-4-phenyl-1,2,3,6-tetrahydropyridine (MPTP) and rotenone, have been reported to lead to the degeneration of dopaminergic neurons in the substantia nigra pars compacta[9,10] by inhibiting mitochondrial complex I in the electron transfer chain and subsequently increasing the generation of ROS.[2,5,11,12] Furthermore, MPP$^+$, the oxidized product of MPTP, decreased mitochondrial activity and mitochondrial gene expressions in neuronal cells, similar to MPTP treatment *in vivo*.[13] However, our understanding of the exact molecular mechanisms that underlie PD remains incomplete.

Recently, several proteomic studies have been performed to investigate alterations in protein levels.[14] To date, two-dimensional gel electrophoresis (2-DE) has mainly been used to study protein alterations associated with PD.[7,15] These 2-DE based proteomic techniques have several disadvantages, namely, the detection of changes only in abundantly expressed proteins and the inability to analyze extremely low or high molecular weight proteins.[16] These studies have shown identification of the small number of differentially expressed proteins in the MPP$^+$ treated SH-SY5Y cells (9 proteins by Davison *et al.*,[17] and 22 by Xie *et al.*[7]). On the other hand, we identified more than total 1700 proteins using the LC coupled with the MS system in MPP$^+$-treated SH-SY5Y cells, 39 of which were differentially expressed.

In the present study, we performed a large scale proteomic study using stable isotope labeling with amino acids in cell culture (SILAC) combined with nano-LC tandem mass spectrometry

[a] *Department of Physiology, Kyung Hee University School of Medicine, 26 Kyungheedae-ro, Dondaemun-gu, Seoul 130-701, South Korea. E-mail: kspark@khu.ac.kr; Fax: +82-2-964-2195; Tel: +82-2-961-0292*
[b] *Biomedical Science Institute, Kyung Hee University School of Medicine, Seoul 130-701, South Korea*

† Electronic supplementary information (ESI) available. See DOI: 10.1039/c4mb00026a

(nano-LC-MS) to identify differentially expressed proteins in MPP^+-treated SH-SY5Y cells. With this method, we have not only confirmed the previously reported proteins associated with PD but have also identified new proteins linked to PD. Our study offers new insights into the potential functional mechanisms involved in PD.

Materials and methods

Cell culture

SH-SY5Y cells were maintained in Dulbecco's modified Eagle's medium (DMEM) supplemented with 10% fetal bovine serum (FBS; Invitrogen, NY, USA), 100 U mL^{-1} penicillin, and 100 mg mL^{-1} streptomycin. Cells in the log phase were used for the experiments.

SILAC and MPP^+ treatment

SILAC was performed as reported previously.[18] Briefly, SH-SY5Y cells were grown for at least five cell divisions in either "light" SILAC media containing $^{12}C_6$-Arg and $^{12}C_6$, $^{14}N_2$-Lys or "heavy" SILAC media containing $^{13}C_6$-Arg and $^{13}C_6$, $^{15}N_2$-Lys supplemented with 10% dialyzed FBS, 50 IU mL^{-1} penicillin, and 50 mg mL^{-1} streptomycin. MPP^+ was added at a final concentration of 1 mM to the dish of heavy-labeled cells and incubated for 24 h. The cells in both dishes were then lysed in buffer containing 1% Triton X-100, 150 mM NaCl, 1 mM EDTA, 50 mM Tris-HCl (pH 8.0), 1 mM sodium orthovanadate, 5 mM NaF, 5 mM sodium pyrophosphate, 1 mM PMSF, aprotinin (1.5 μg mL^{-1}), antipain (10 μg mL^{-1}), leupeptin (10 μg mL^{-1}), and benzamidine (0.1 mg mL^{-1}). The lysates were centrifuged at 160 000 × *g* and combined in a 1 : 1 ratio according to their protein concentration, which was estimated using the BCA assay (Pierce, Rockford, IL). The mixed lysates were separated *via* 10% SDS-PAGE and visualized by staining with Coomassie Brilliant Blue G-250.

In-gel digestion

Each gel was directly cut into ten bands of equal size, de-stained with 50% acetonitrile in 25 mM ammonium bicarbonate and dried in a speed vacuum concentrator. Dried gel pieces were re-swollen using 25 mM ammonium bicarbonate (pH 8.0) containing 50 ng trypsin and incubated at 37 °C for 16–24 h. Supernatant peptide mixtures were extracted with 50% acetonitrile in 5% formic acid and dried in a speed vacuum concentrator.

Mass spectrometry analysis

The tryptic-dried samples were analyzed using the Agilent HPLC-Chip/TOF MS system with the Agilent 1260 nano-LC system, HPLC Chip-cube MS interface and a 6530 QTOF single quadrupole-TOF mass spectrometer (Agilent Technologies, Santa Clara, CA). The dried peptide samples were re-suspended in 2% ACN/0.1% FA and concentrated on a large-capacity HPLC Chip (Agilent Technologies). The HPLC chip incorporated an enrichment column (9 mm, 75 μm I.D., 160 nl) and a reverse-phase column (15 cm, 75 μm I.D., packed with Zorbax 300SB-C18 5 μm resins).

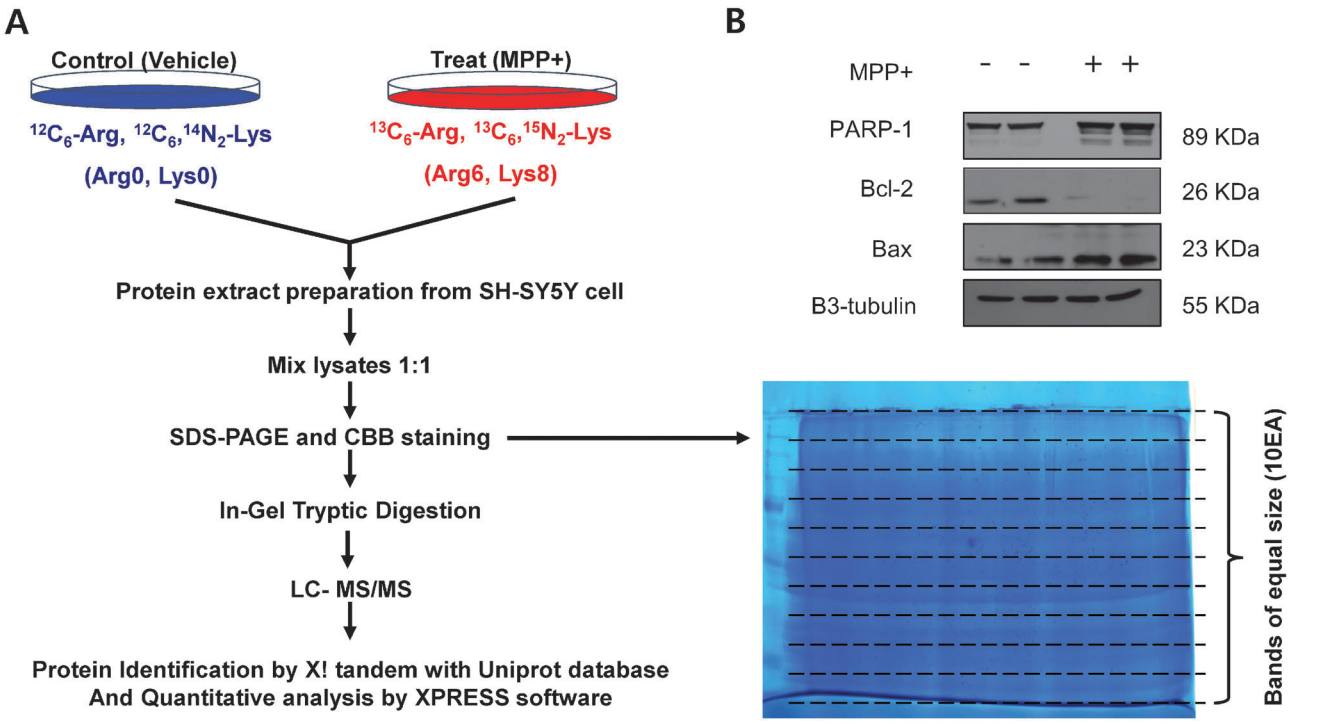

Fig. 1 SILAC analysis and characterization of MPP^+-treated SH-SY5Y cells. (A) Schematic outline of the SILAC experiments to quantify protein changes in MPP^+-treated SH-SY5Y cells. SH-SY5Y cells were treated with MPP^+ for 24 h to induce apoptotic cell death. Each sample was lysed and separated *via* 10% SDS-PAGE, followed by in-gel tryptic digestion. The tryptic peptide mixtures were analyzed by mass spectrometry. (B) Immunoblot analysis of MPP^+-induced apoptosis in SH-SY5Y cells. PARP-1 cleavage, decreased Bcl-2, and increased Bax were observed after MPP^+ treatment.

The peptide separation was performed using a 110 min gradient of 3–45% buffer B (buffer A contained 0.1% FA, and buffer B contained 90% ACN/0.1% FA) at a flow rate of 300 nl min^{-1}. The MS and MS/MS data were acquired in the positive ion mode and data stored centroid mode. The chip spray voltage was set at 1850 V and maintained under chip conditions. The drying gas temperature was set at 325 with a flow rate of 3.5 l min^{-1}. A medium isolation (4 m/z) window was used for precursor isolation. Collision energy with a slope of 3.7 V/100 Da and an offset of 2.5 V were used for fragmentation. Additionally, while the MS data were acquired over a mass range of 300–3000 m/z, the MS/MS data were acquired over a 50–2500 m/z mass range. Reference mass correction was performed using a reference mass of 922. Precursors were set in an exclusion list for 0.5 min after two MS/MS spectra. The MS/MS spectra were extracted using the MassHunter Qualitative Analysis B.05.00 software (Agilent Technologies, Santa Clara, CA) with default parameters. Protein identification was performed with the X! Tandem search engine by searching against the Uniprot database. Database searches were performed with a peptide mass tolerance of 20 ppm, an MS/MS tolerance of 0.5 Da, and a strict tryptic specificity (cleavage after lysine and arginine) allowing one missed cleavage site; carbamidomethylation of Cys was set as a fixed modification, whereas oxidation (M) was considered a variable modification.

Protein validation and quantification

X! tandem search result files were analyzed using the Trans-Proteomic Pipeline (TPP) (Systems Biology, Seattle, WA). All assigned peptides were validated by PeptideProphet[19] and the results filtered by an error rate of 0.05 (FDR 5%). Peptide quantification analysis was performed using the XPRESS[20] modules included in the TPP. Protein identification and quantification were validated using ProteinProphet[21] and the result cutoff was set to the protein probability of 80%/error rate of 0.05 (FDR 5%) and a ratio of light from fixed to 1. SILAC ratios for proteins were quantified using the XPRESS software. The elution profiles of the light and heavy

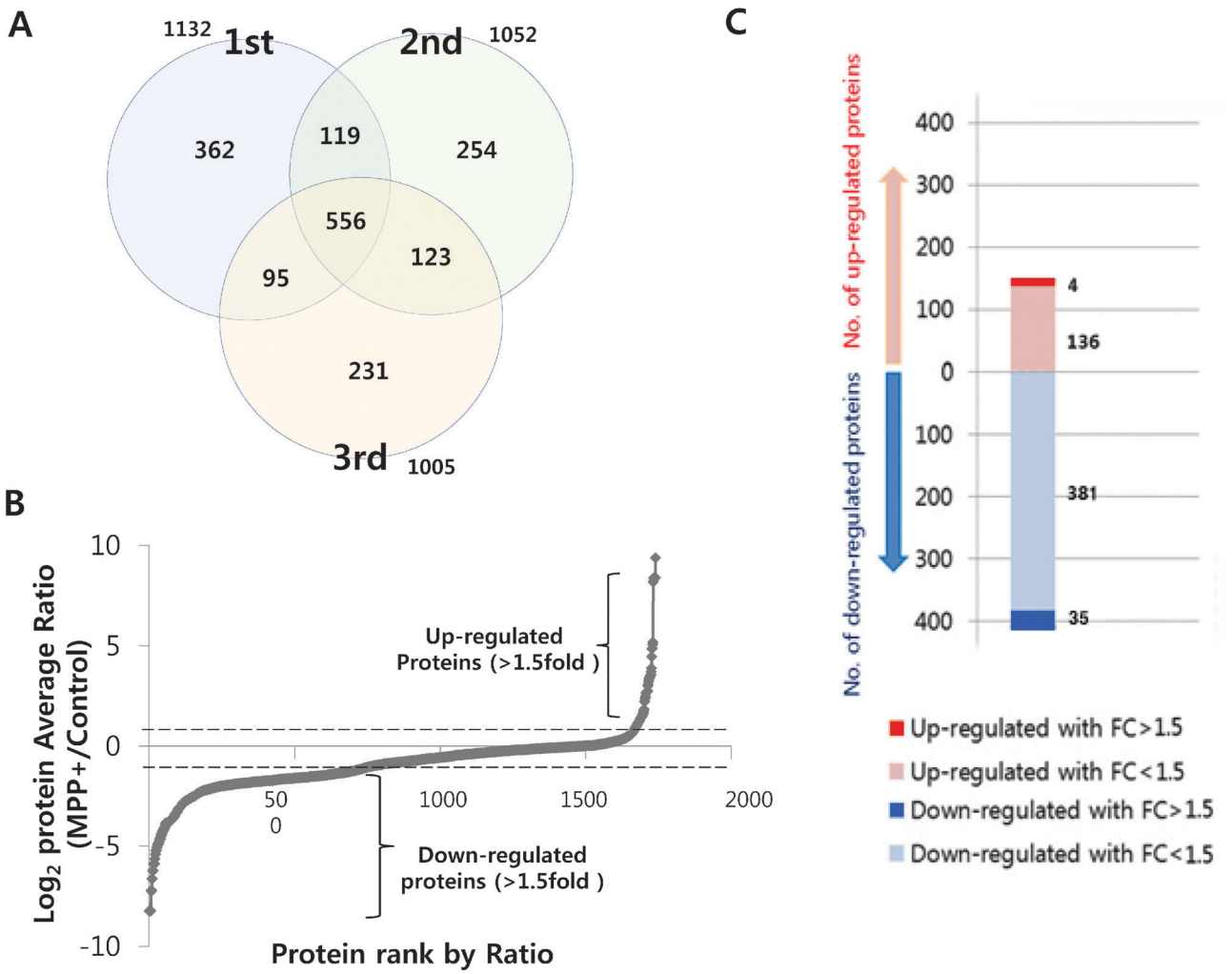

Fig. 2 Quantitative analysis of the proteins identified in MPP^+-induced apoptosis. (A) The Venn diagram shows the overlap between the proteins identified in three independent biological replicates after MPP^+-induced apoptosis. A total of 1740 proteins were identified from the three replicates, and 556 proteins overlapped. (B) Ratio distribution of identified proteins in MPP^+-treated SH-SY5Y cells. (C) Distribution of differentially expressed proteins. Red and blue bars show proteins that were significantly up-regulated and down-regulated, respectively. A total of 39 proteins were either up- or down-regulated by >1.5 fold in MPP^+-treated SH-SY5Y cells.

peptides were isolated and quantified based on the area of each peptide peak and calculated the abundance ratio based on these areas by XPRESS. Quantitative protein ratios were determined by the average level of quantified peptides.

Bioinformatics analysis

Gene Ontology (GO) analysis was performed using Cytoscape and the Plugin ClueGO, and pathway analysis was performed using the KEGG pathway database and ProteinCenter (Thermo Scientific, Denmark) web-based software. Functional protein–protein network analysis was performed using STRING.

Results and discussion

To further investigate the potential mechanisms of PD, we performed global proteomic profiling of SH-SY5Y cells after MPP^+ treatment using SILAC combined with nano-LC mass spectrometry (Fig. 1A). SH-SY5Y cells were cultured in either "light" SILAC media containing $^{12}C_6$-Arg and $^{12}C_6$, $^{14}N_2$-Lys or "heavy" SILAC media containing $^{13}C_6$-Arg and $^{13}C_6$, $^{15}N_2$-Lys until cells were fully labeled with the stable isotopes. Cells grown in "light" media were treated with vehicle, whereas cells grown in "heavy" media were treated with MPP^+. Consistent with previous results,[22] MPP^+ treatment resulted in PARP-1 cleavage, decreased Bcl-2 levels, and increased Bax levels, all of which are markers for MPP^+-induced apoptosis (Fig. 1B). These results indicate that MPP^+-induced apoptosis was efficiently established in this study.

Three independent SILAC experiments were performed with MPP^+ treated SH-SY5Y cells. Protein lysates were mixed in a 1 : 1 ratio and run on SDS-PAGE gels, and 10 bands were excised and in-gel digested. Tryptic peptides were then subjected to nano LC-mass spectrometry. Only proteins detected with paired light- and heavy-labeled peptides were included in the three independent datasets. A total of 1740 proteins were identified and quantified from three independent replicates (ESI,† Table S1), and 556 overlapping proteins were detected from the three datasets (Fig. 2A). For quantitative analysis, protein ratios were calculated using XPRESS software by comparing the extract ion chromatography of the light- and heavy-labeled peptides from tandem mass spectrometry and applying a fold-change cutoff of >1.5 for further analyses. Proteins not commonly detected in the three independent replicates were excluded from our dataset. Of the quantified proteins, 93% showed a change of less than 1.5 fold (Fig. 2B). However, 4 proteins were up-regulated by more than 1.5 fold, and

Table 1 List of significantly down-regulated proteins with a >1.5-fold change

Accession	Gene name	Protein description	Log2 ratio (treat/control)
P0C7U0	PPR28	Protein phosphatase 1 regulatory subunit 28	−1.84
P09001	MRPL3	39S ribosomal protein L3	−1.43
Q15046-2	KARS	Isoform mitochondrial of lysine-tRNA ligase	−1.40
P04908	H2A1B	Histone H2A type 1-B/E	−1.27
Q5JTZ9	AARS2	Alanine-tRNA ligase	−1.21
Q15056-2	IF4H	Isoform short of eukaryotic translation initiation factor 4H	−1.06
P25325	MPST	3-Mercaptopyruvate sulfurtransferase	−1.02
Q16763	UBE2S	Ubiquitin-conjugating enzyme E2 S	−1.01
O75489	NDUS3	NADH dehydrogenase [ubiquinone] iron–sulfur protein 3	−0.95
Q08J23-2	NSUN2	Isoform 2 of tRNA (cytosine(34)-C(5))-methyltransferase	−0.94
P28161	GSTM2	Glutathione *S*-transferase Mu 2	−0.89
Q8NBX0	SCPDL	Saccharopine dehydrogenase-like oxidoreductase	−0.86
P00403	COX2	Cytochrome *c* oxidase subunit 2	−0.85
P13796	PLSL	Plastin-2	−0.84
Q16795	NDUA9	NADH dehydrogenase [ubiquinone] 1 alpha subcomplex subunit 9	−0.80
Q9GZR7	DDX24	ATP-dependent RNA helicase DDX24	−0.79
O15020-2	SPTN2	Isoform 2 of spectrin beta chain	−0.76
Q7Z7H8	MRPL10	39S ribosomal protein L10	−0.75
P62314	SMD1	Small nuclear ribonucleoprotein Sm D1	−0.71
O96008	TOMM40	Mitochondrial import receptor subunit TM40 homolog	−0.71
P05386	RLA1	60S acidic ribosomal protein P1	−0.70
P20290-2	BTF3	Isoform 2 of transcription factor BTF3	−0.69
O43809	CPSF5	Cleavage and polyadenylation specificity factor subunit 5	−0.69
Q9BPW8	NIPSNAP1	Protein NipSnap homolog 1	−0.67
Q9Y277-2	VDAC3	Isoform 2 of voltage-dependent anion-selective channel protein 3	−0.64
Q7Z4W1	DCXR	L-Xylulose reductase	−0.63
Q01518	CAP1	Adenylyl cyclase-associated protein 1	−0.62
Q16363-2	LAMA4	Isoform 2 of laminin subunit alpha-4	−0.62
P24539	AT5F1	ATP synthase subunit b	−0.62
Q99714	HSD17B10	3-Hydroxyacyl-CoA dehydrogenase type-2	−0.62
O60814	H2B1K	Histone H2B type 1-K	−0.61
Q00534	CDK6	Cyclin-dependent kinase 6	−0.59
P08621-2	RU17	Isoform 2 of U1 small nuclear ribonucleoprotein 70 kDa	−0.58
Q9ULC4-2	MCTS1	Isoform 2 of malignant T-cell-amplified sequence 1	−0.58
P08670	VIME	Vimentin	−0.58

Accession #s are from the Uniprot database; significantly different protein modulations ($p < 0.05$); fold change is calculated using MPP^+ treated/control (unlabeled/labeled) ratios quantitated from integrated proteomics software. Ratios were obtained from $n = 3$.

Table 2 List of significantly up-regulated proteins with >1.5-fold change

Accession	Gene name	Protein description	Log2 ratio (treat/control)
Q9P035	HACD3	3-Hydroxyacyl-CoA dehydratase 3	0.60
P08243	ASNS	Asparagine synthetase [glutamine-hydrolyzing]	0.73
Q12874	SF3A3	Splicing factor 3A subunit 3	1.08
G3V2J8	G3V2J8	Heat shock protein HSP 90-alpha (fragment)	2.62

Accession #s are from the Uniprot database; significantly different protein modulations ($p < 0.05$); fold change is calculated using MPP^+ treated/control (unlabeled/labeled) ratios quantitated from integrated proteomics software. Ratios were obtained from $n = 3$.

35 proteins were down-regulated by more than 1.5 fold in MPP^+-treated SH-SY5Y cells (Fig. 2C and Tables 1 and 2).

Fig. 3A shows the Gene Ontology (GO) distributions as a pie chart for the biological processes significantly enriched in the dataset. Cellular component term annotation-predicted cellular localization reveals that most proteins were associated with cytoplasm-, nucleus-, cytosol-, organelle lumen-, and membrane-related GO terms. In the biological process category, most proteins were involved in metabolic processes, cell organization and biogenesis, responses to stimulus, and transport, for which 13 subcategory terms were identified. The molecular function category showed that proteins related to binding and catalytic activity were most frequent, and 12 subcategory terms were identified. KEGG pathway analysis of all identified proteins was performed based on signaling pathways. Pathways mainly associated with protein (ribosome and proteasome), RNA (spliceosome and aminoacyl-tRNA biosynthesis), and metabolism (carbon metabolism, pyruvate metabolism, glycolysis/gluconeogenesis, and citrate cycle) were enriched in the MPP^+-induced apoptotic cells (Fig. 3B). Interestingly, PD was significantly identified through the KEGG pathway analysis (ESI,† Fig. S1). In total, 20 proteins were matched onto the PD pathway containing well known proteins associated with PD (Table 3).

Next, to explore biological functions and pathways playing a critical role in PD, we performed bioinformatic analyses of the proteins differentially expressed in response to MPP^+-induced apoptosis. KEGG pathway analysis of the differentially expressed proteins indicated that the most relevant pathways were as follows: PD, oxidative phosphorylation, Alzheimer's disease, Huntington's disease, and systemic lupus erythematosus (Fig. 4A). Interestingly, PD was the top altered pathway. Cellular localization analysis using

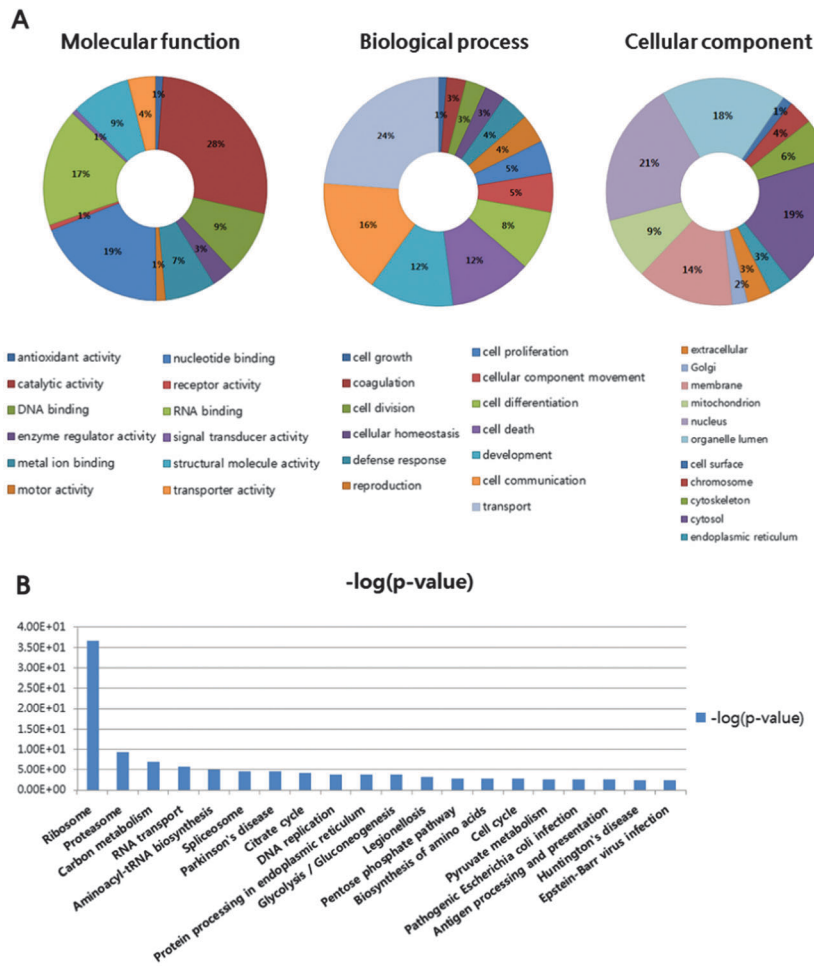

Fig. 3 Characterization of proteins by GO term annotation and the KEGG pathway. (A) The identified proteins were categorized by molecular function, biological process and cellular component using GO annotation. (B) KEGG pathway analysis of all identified proteins.

Table 3 List of proteins matched with Parkinson's disease pathway using KEGG database

Accession	Gene name	Protein description
P24539	AT5F1	ATP synthase subunit b
P48047	ATPO	ATP synthase subunit O
P25705	ATPA	ATP synthase subunit alpha
P06576	ATPB	ATP synthase subunit beta
P36542	ATPG	Isoform heart of ATP synthase subunit gamma
P00403	COX2	Cytochrome *c* oxidase subunit 2
Q16795	NDUA9	NADH dehydrogenase [ubiquinone] 1 alpha subcomplex subunit 9
O75489	NDUS3	NADH dehydrogenase [ubiquinone] iron–sulfur protein 3
O00217	NDUS8	NADH dehydrogenase [ubiquinone] iron–sulfur protein 8
Q99497	PARK7	Protein DJ-1
P99999	CYC	Cytochrome *c*
P05141	ADT2	ADP/ATP translocase 2
P31040	DHSA	Succinate dehydrogenase [ubiquinone] flavoprotein subunit
P31930	QCR1	Cytochrome *b*-*c*1 complex subunit 1
P22695	QCR2	Cytochrome *b*-*c*1 complex subunit 2
P09936	UCHL1	Ubiquitin carboxyl-terminal hydrolase isozyme L1
P22314	UBA1	Ubiquitin-like modifier-activating enzyme 1
P21796	VDAC1	Voltage-dependent anion-selective channel protein 1
P45880	VDAC2	Isoform 1 of voltage-dependent anion-selective channel protein 2
Q9Y277	VDAC3	Isoform 2 of voltage-dependent anion-selective channel protein 3

Accession #s are from the Uniprot database; significantly different protein modulations ($p < 0.05$); fold change is calculated using MPP^+ treated/control (unlabeled/labeled) ratios quantitated from integrated proteomics software. Ratios were obtained from $n = 3$.

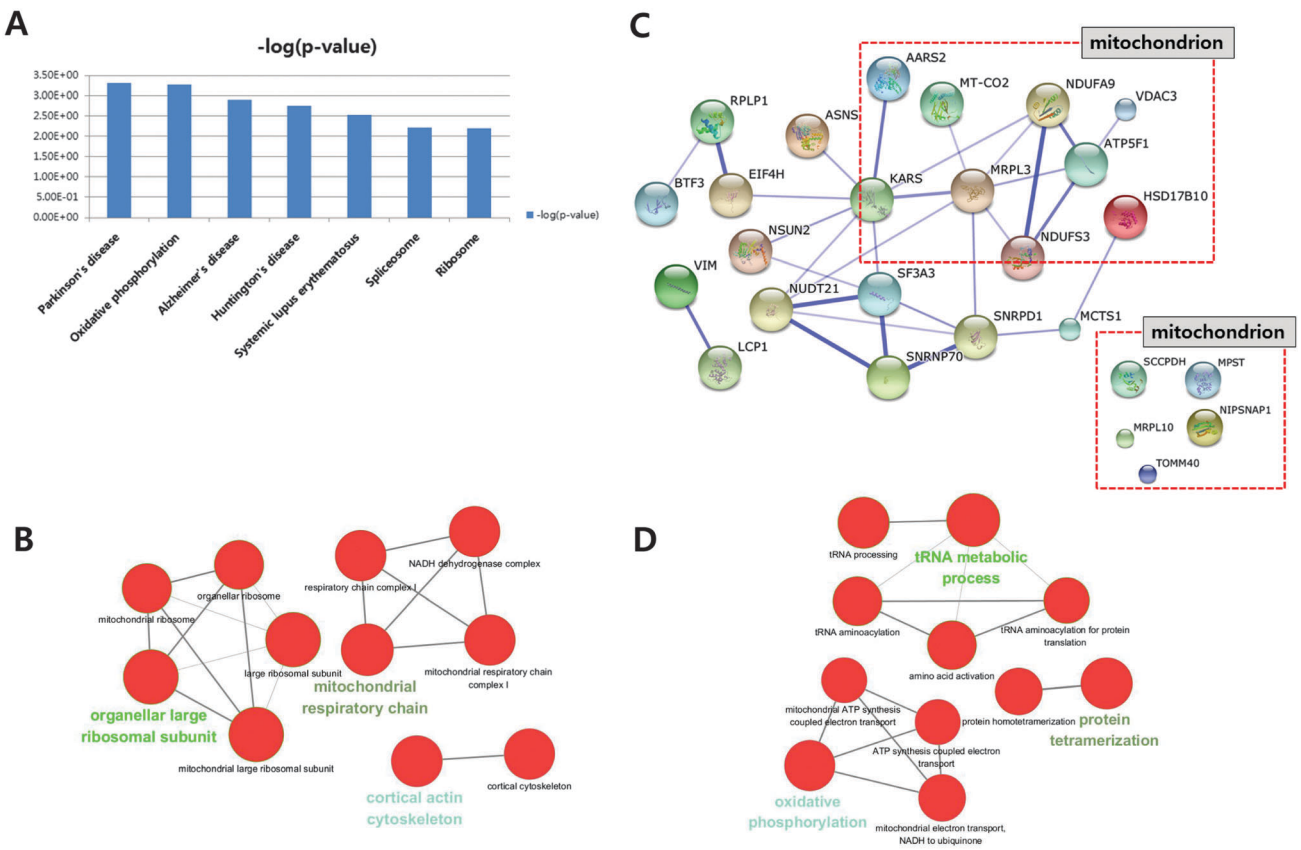

Fig. 4 KEGG pathway and GO annotation analysis of proteins altered by >1.5 fold. (A) KEGG pathway analysis of the differentially expressed proteins in MPP^+-treated SH-SY5Y cells. Pathways were considered significant based on *p*-value enrichment. (B) GO cellular component network comparing the classifications of altered proteins from MPP^+-treated SH-SY5Y cells. GO cellular components were assigned by the ClueGo Cytoscape plugin. (C) Protein–protein interaction networks were visualized using STRING web-based software. Protein–protein interaction networks containing differentially expressed proteins with a >1.5-fold change. Proteins were divided into several groups depending on their features. Circles represent each protein, and the thickness of the blue lines indicates interrelationships between the proteins. Proteins with dashed lines are localized in the mitochondria. (D) GO biological process network comparing the classifications of altered proteins in MPP^+-treated SH-SY5Y cells. GO biological processes were assigned by the ClueGo Cytoscape plugin.

GO terms assigned by the ClueGO Cytoscape plugin showed that proteins associated with the mitochondria were critically affected by MPP^+-induced apoptosis. In fact, 35% of the altered proteins were related to the mitochondria (Fig. 4B), which are significantly associated with PD.[22,23] It has been reported that MPP^+-induced apoptosis leads to proteasome dysfunction, inhibition of mitochondrial complex I, and increased oxidative stress.[2,5,9,24] These pathogenic pathways are commonly associated with mitochondrial activity, potentially impairing proteasomal function. In addition, we noted the protein–protein interaction network between the altered proteins using STRING web-based software. Analysis of protein–protein interaction network positions revealed that proteins located in the network were mitochondrial proteins (Fig. 4C). A total of 14 mitochondrial proteins were found with a main network position (AARS2, ATP5F1, NDUFA9, NDUFS3, VDAC3, KARS, MRPL3, COX2, HSD17B10, TOMM40, MPST, NIPSNAP1, MRPL10, and SCCPDH). Interestingly, among these mitochondrial proteins, 5 proteins (ATP5F1, NDUFA9, NDUFS3, VDAC3, and COX2) have been reported to be associated with PD. NDUFA9 and NDUFS3 are known to be subunits of complex I. MPTP reduces the level of functional CI in the electron transport system by inhibiting NAD(H)-linked mitochondrial oxidation.[1] VDAC3 is essential for the recruitment of Parkin from the cytosol to defective mitochondria.[9] It has been reported that ATP5F1, which belongs to the mitochondrial oxidative phosphorylation system, is associated with PD.[1] The role of COX2 has been well studied in PD.[5] Therefore, these results showed that our method combining SILAC with nano LC-MS is a useful approach for investigating the proteome associated with PD.

Interestingly, using the ClueGO Cytoscape plugin indicated that these proteins were enriched in GO biological processes associated with tRNA metabolism, as well as oxidative phosphorylation (Fig. 4D). The AARS2, HSD17B10, and KARS proteins involved in the tRNA metabolic process have been shown to be associated with angiogenesis, apoptosis, and Parkinson's disease.[6,25–27]Although these proteins have previously been shown to be involved in various pathogenic conditions, little is known regarding their roles in PD. Similar to the tRNA metabolism proteins, the MRPL3 and MRPL10, TOMM40, MPST, NIPSNAP1, and SCCPDH proteins, which are thought to be linked to many human diseases, were observed as well.[2,28] However, the relevance of these proteins to PD is not yet clear. Therefore, these mitochondrial proteins may be candidate proteins related to the functional mechanisms of PD.

Conclusion

Many studies have been performed to gain more insight into the molecular mechanism of PD. Previous studies have used 2DE-based proteomics analysis to investigate differentially expressed proteins associated with PD. Despite these efforts, and due to the limitations of gel-based proteomics tools, a number of questions still remain about the potential functional mechanisms of PD. In this study, we used large-scale, high-resolution MS-based proteomics technology combined with SILAC for analysing MPP^+-induced apoptosis in SH-SY5Y cells. A total of 1740 proteins were identified from the three biological replicates, and our comparative proteomic analysis revealed that a total of 39 proteins were differentially expressed in SH-SY5Y cells responding to the MPP^+ treatment. Interestingly, 14 of these proteins are localized to the mitochondria, and a further 5 proteins were already reported to be related to PD. Moreover, 9 of the altered mitochondrial proteins have not been previously reported and might therefore be candidates for determining the molecular mechanism of PD. Altogether, our data further affirm the important roles that mitochondrial proteins play in regulating PD through multiple and complex mechanisms. Further studies are needed to determine whether the candidate proteins identified in this study might be new targets for understanding the potential mechanisms of PD.

Acknowledgements

This research was supported by a Kyung Hee University Research Grant (KHU-20100854).

References

1 P. C. Keane, M. Kurzawa, P. G. Blain and C. M. Morris, *Parkinson's Dis.*, 2011, **2011**, 716871.
2 S. E. Calvo and V. K. Mootha, *Annu. Rev. Genomics Hum. Genet.*, 2010, **11**, 25–44.
3 S. R. Subramaniam and M. F. Chesselet, *Prog. Neurobiol.*, 2013, **106–107**, 17–32.
4 D. N. Hauser and T. G. Hastings, *Neurobiol. Dis.*, 2013, **51**, 35–42.
5 P. Teismann, *BioFactors*, 2012, **38**, 395–397.
6 S. G. Park, P. Schimmel and S. Kim, *Proc. Natl. Acad. Sci. U. S. A.*, 2008, **105**, 11043–11049.
7 H. Xie, M. Chang, X. Hu, D. Wang, M. Tian, G. Li, H. Jiang, Y. Wang, Z. Dong, Y. Zhang and L. Hu, *Neurol. Sci.*, 2011, **32**, 221–228.
8 V. Bonifati, P. Rizzu, M. J. van Baren, O. Schaap, G. J. Breedveld, E. Krieger, M. C. Dekker, F. Squitieri, P. Ibanez, M. Joosse, J. W. van Dongen, N. Vanacore, J. C. van Swieten, A. Brice, G. Meco, C. M. van Duijn, B. A. Oostra and P. Heutink, *Science*, 2003, **299**, 256–259.
9 Y. Sun, A. A. Vashisht, J. Tchieu, J. A. Wohlschlegel and L. Dreier, *J. Biol. Chem.*, 2012, **287**, 40652–40660.
10 H. B. Pollard, G. A. Kuijpers, O. M. Adeyemo, M. B. Youdim and G. Goping, *Exp. Neurol.*, 1996, **142**, 170–178.
11 S. M. Heman-Ackah, M. Hallegger, M. S. Rao and M. J. Wood, *Front. Mol. Neurosci.*, 2013, **6**, 40.
12 R. Perfeito, T. Cunha-Oliveira and A. C. Rego, *Free Radical Biol. Med.*, 2013, **62**, 186–201.
13 A. Aggarwal, D. J. Schneider, E. F. Terrien, C. M. Terrien, Jr., B. E. Sobel and H. L. Dauerman, *Am. J. Cardiol.*, 2003, **91**, 1346–1349.
14 M. Shi, W. M. Caudle and J. Zhang, *Neurobiol. Dis.*, 2009, **35**, 157–164.

15 Y. Zhang, H. Wang, C. Lai, L. Wang and Y. Deng, *Astrobiology*, 2013, **13**, 143–150.
16 P. Sharma, J. Cosme and A. O. Gramolini, *J. Proteomics*, 2013, **81**, 3–14.
17 E. J. Davison, K. Pennington, C. C. Hung, J. Peng, R. Rafiq, A. Ostareck-Lederer, D. H. Ostareck, H. C. Ardley, R. E. Banks and P. A. Robinson, *Proteomics*, 2009, **9**, 4284–4297.
18 K. S. Park, D. P. Mohapatra, H. Misonou and J. S. Trimmer, *Science*, 2006, **313**, 976–979.
19 A. Keller, A. I. Nesvizhskii, E. Kolker and R. Aebersold, *Anal. Chem.*, 2002, **74**, 5383–5392.
20 D. K. Han, J. Eng, H. Zhou and R. Aebersold, *Nat. Biotechnol.*, 2001, **19**, 946–951.
21 A. I. Nesvizhskii, A. Keller, E. Kolker and R. Aebersold, *Anal. Chem.*, 2003, **75**, 4646–4658.
22 C. Perier, J. Bove and M. Vila, *Antioxid. Redox Signaling*, 2012, **16**, 883–895.
23 W. J. Nicklas, S. K. Youngster, M. V. Kindt and R. E. Heikkila, *Life Sci.*, 1987, **40**, 721–729.
24 L. Villeneuve, L. M. Tiede, B. Morsey and H. S. Fox, *J. Proteome Res.*, 2013, **12**, 4599–4606.
25 D. K. Simon, R. Mayeux, K. Marder, N. W. Kowall, M. F. Beal and D. R. Johns, *Neurology*, 2000, **54**, 703–709.
26 R. Egensperger, S. Kosel, N. M. Schnopp, P. Mehraein and M. B. Graeber, *Neuropathol. Appl. Neurobiol.*, 1997, **23**, 315–321.
27 U. Mayr-Wohlfart, G. Rodel and A. Henneberg, *Eur. J. Med. Res.*, 1997, **2**, 111–113.
28 E. Tolkunova, H. Park, J. Xia, M. P. King and E. Davidson, *J. Biol. Chem.*, 2000, **275**, 35063–35069.